
Stochastically Dominant Distributional Reinforcement Learning

John D. Martin Michal Lyskawinski Xiaohu Li Brendan Englot
Stevens Institute of Technology
{jmarti3, mlyskawi, xli82, benglot}@stevens.edu

Abstract

We describe a new approach for mitigating risk in the Reinforcement Learning paradigm. Instead of reasoning about expected utility, we use second-order stochastic dominance (SSD) to directly compare the dispersion of random returns induced by different actions. We frame the RL optimization within the space of probability measures to accommodate the SSD relation, treating the distributional Bellman equation as a potential energy functional. This brings us to Wasserstein gradient flows, under which we prove optimality and convergence of our solutions. We propose a discrete-measure approximation algorithm called the Dominant Particle Agent (DPA), and we demonstrate how safety and performance are better balanced with DPA using SSD action selection than with other risk metrics.

1 Introduction

As rational agents operating in a stochastic world, Reinforcement Learning (RL) agents prefer actions of the greatest expected utility, or return (Sutton and Barto, 1998; von Neumann and Morgenstern, 1947). Naturally any decision comes with the possibility of an undesirable outcome. To avoid risky outcomes, utility functions are often adjusted to shift preferences away from uncertainty and toward choices with greater predictability (Borkar, 2002; Fishburn, 1964). In this paper we remove the need for an explicit utility function and instead reason about risk on a more intrinsic level. Specifically, we employ the second-order stochastic dominance (SSD) relation to define a new policy, directly comparing the underlying risk of random returns induced by actions.

The SSD relation is defined using distribution functions and compared over the continuum of their realizable values. We say that X stochastically dominates Y in the second order when the integrated CDFs, $F^{(2)}(\alpha) = \int_{-\infty}^{\alpha} F(x)dx$, satisfy (1), and we denote the relation $X \succeq_{(2)} Y$:

$$X \succeq_{(2)} Y \iff F_X^{(2)}(\alpha) \leq F_Y^{(2)}(\alpha) \forall \alpha \in \mathbb{R}. \quad (1)$$

The function $F^{(2)}$ defines the frontier of what is known as the *dispersion space* (Figure 1). The volume reflects the degree to which a random variable differs from its deterministic behavior - if it were simply equal to its mean with no uncertainty. Outcomes that are disperse are considered risky. Hence, rational risk-averse agents prefer X to Y when $X \succeq_{(2)} Y$. Our paper draws inspiration from this decision strategy (Dentcheva and Ruszczyński, 2006) to propose a safer means of exploration. We offer the following contributions:

A comprehensive risk metric: RL methods typically measure uncertainty with the return distribution’s variance (Markowitz, 1952; Sato et al., 2001; Tamar et al., 2013), or with quantile risk measures (Chow and Ghavamzadeh, 2014; Chow et al., 2017; Morimura et al., 2010). Interestingly, we can show these are all special cases of SSD, and that they are less accurate measures of risk. Because SSD captures all the distributional geometry, it can detect unfavorable outcomes other metrics miss.

A risk-aware policy for Distributional RL: We use the SSD relation to define a new risk-sensitive exploration policy, whereby the agent acts according to the least-disperse return distribution. When evaluating exploratory actions, the agent breaks ties with dispersion for improved safety.

New language to understand Distributional RL: Our agent learns distributions over returns for each action. Learning is made possible through the class of Distributional RL algorithms, described by Bellemare et al. (Bellemare et al., 2017). These algorithms model a distribution over the return, whose mean is the familiar value function, and use it to evaluate and optimize a policy (Barth-Maron et al., 2018; Hessel et al., 2018).

Methods that use particle (quantile) models have shown encouraging progress on empirical benchmarks (Dabney et al., 2018, 2017), but understanding their convergence has been more challenging. By casting the optimization problem as free-energy minimization in the space of probability measures, we show that solutions evolve as a Wasserstein Gradient Flow (WGF) (Ambrosio, 2005). Model updates in this framework have well-determined dynamics. And under certain conditions, which we detail in Section 3, we are able to prove convergence. Our empirical results validate the new WGF learning framework and show that it is possible to simultaneously learn optimal return distributions and balance risk with SSD action selection.

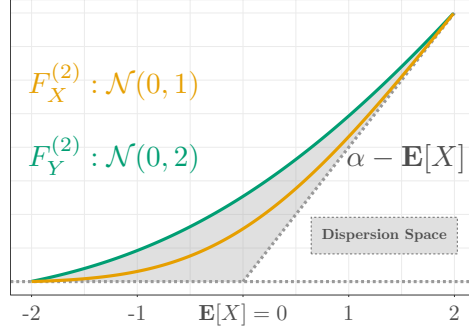


Figure 1: **Dispersion space:** The uncertainty (risk) of a random variable is shown as the space between its cumulative CDF $F^{(2)}$ and the asymptotes (dotted). Here, the line $\alpha - \mathbf{E}[X]$ defines the behavior of X as its uncertainty vanishes.

2 Reinforcement Learning Preliminaries

Reinforcement Learning describes a sequential decision making problem, whereby an agent learns to act optimally from rewards collected after taking actions (Sutton and Barto, 1998). The *random return* defines optimality:

$$Z_{\pi}^{(s,a)} = \sum_{t=0}^{\infty} \gamma^t R^{(S_t, A_t)} \Big| S_0 = s, A_0 = a. \quad (2)$$

It reflects the outcome of a decision sequence that starts after taking action $a \in \mathcal{A}$ in state $s \in \mathcal{S}$, then following the policy $\pi \in \Pi$ thereafter. Policies are stationary distributions over actions, coming from the set $\Pi = \{\pi | \pi: \mathcal{S} \rightarrow \mathcal{P}(\mathcal{A})\}$. Here, $\gamma \in [0, 1]$ is a discount factor, and $R^{(S_t, A_t)}$ is the real-valued random reward associated with state S_t and action A_t .

At each time step, the agent selects an action based on its current state, then transitions to the next state and collects a reward. Formally, the interaction is modeled as a Markov Decision Process (MDP), associated with the transition kernel $p: \mathcal{S} \times \mathcal{A} \rightarrow \mathcal{P}(\mathbb{R} \times \mathcal{S})$, which defines a joint distribution over the reward and next state, given the current state-action pair. Here, \mathcal{S} and \mathcal{A} are measurable Borel subsets of complete and separable metric spaces, which we take as finite. And for each state $s \in \mathcal{S}$, the set $\mathcal{A}_s \subset \mathcal{A}$ is a measurable set indicating the feasible actions from s .

2.1 Bellman's Equation

The expected return $\mathbf{E}_{\mu^{(s,a)}}[Z_{\pi}^{(s,a)}] = Q_{\pi}^{(s,a)}$ obeys a recursive decomposition (Bellman, 1957) known as Bellman's equation:

$$Q_*^{(s,a)} = r^{(s,a)} + \gamma \mathbf{E}_p[Q_*^{(S, a^*)}]. \quad (3)$$

Here, actions are greedy, $a^* \in \arg \max_{a \in \mathcal{A}_s} \mathbf{E}_{\mu}[Z_{\pi}^{(s,a)}]$, and the measure $\mu^{(s,a)} \in \mathcal{P}(\mathbb{R})^{(s,a)}$ captures all possible realizations of the return for a given state-action pair. When possible, we will drop the subscripts and refer to the single measure $\mu^{(s,a)}$ as μ . Viewed as a functional operator, (3) is known to contract to a unique fixed point, Q_* , the optimal value, corresponding to the set of optimal policies $\{\pi_* \in \Pi: \mathbf{E}_{\pi_*}[Q_*^{(s,A)}] = Q_*^{(s,a^*)}, \forall s \in \mathcal{S}\}$. The formula connects the observed reward $r^{(s,a)}$ and

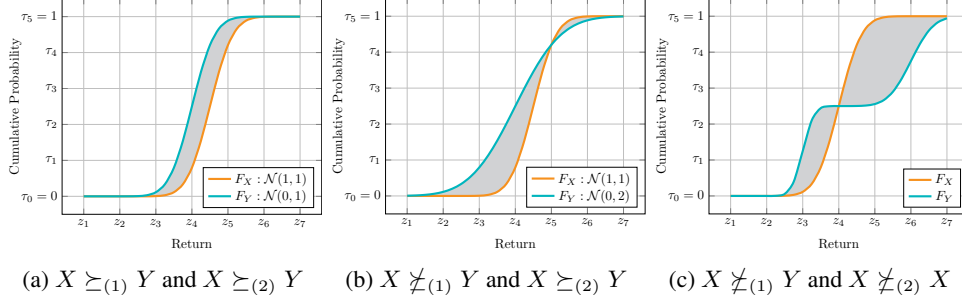


Figure 2: **Stochastic dominance action selection:** Our action selection rule can be visualized with plots of the CDF. In Fig. 2a, $X \succeq_{(1)} Y$, because X places more mass on points larger than α . In Fig. 2b, the area left of z_5 is greater than the area to its right; hence $X \succeq_{(2)} Y$, because the enclosed area is always non-negative. However, in Fig. 2c, neither variable dominates, because after z_4 , the enclosed area becomes negative with respect to X .

latent value, giving rise to many solution methods that update representations of Q to minimize the difference (Bellman error) of both sides (Szepesvári, 2010).

2.2 Distributional Bellman Operators

The return distribution, $\mu^{(s,a)}$, also satisfies a distributional variant of Bellman’s equation:

$$\mathcal{T}^\pi \mu^{(s,a)} = \int_{\mathbb{R}} \sum_{(s',a') \in \mathcal{S} \times \mathcal{A}} f_{\#}^{(r,\gamma)} \mu^{(s',a')} \pi(a'|s') p(dr, s'|s, a). \quad (4)$$

Here, \mathcal{T}^π is the distributional Bellman operator. It embeds a measurable mapping that reflects the Bellman action: $f^{(r,\gamma)}(x) = r + \gamma x$, where the push-forward measure is $f_{\#} \mu^{(A)} = \mu^{(f_{\#}^{-1}(A))} = \nu^{(A)}$, for all Borel measurable sets A . Just as the standard Bellman equation is the focus of standard value-based RL, the distributional Bellman operator (4) plays the central role in Distributional RL; it motivates algorithms which attempt to represent μ and approximate it by repeated application of the update $\mu_{t+1}^{(s,a)} \leftarrow \mathcal{T}^\pi \mu_t^{(s,a)}$, for any $(s, a) \in \mathcal{S} \times \mathcal{A}$ and steps $t = 0, 1, \dots$. The optimal version of the operator is obtained when actions are selected to maximize the expected value:

$$\mathcal{T} \mu^{(s,a)} = \int_{\mathbb{R}} \sum_{(s',a') \in \mathcal{S} \times \mathcal{A}} f_{\#}^{(r,\gamma)} \mu^{(s',a^*)} p(dr, s'|s, a). \quad (5)$$

3 Reducing Risk in Distributional RL

Here we introduce the SSD decision policy (Fig. 2c) as a means to mitigate risk during training. At each state s , the agent compares the relative size of each return distribution’s dispersion. The action inducing a distribution that dominates all the other choices in the second order is considered safest. This corresponds to elements of the set $\mathcal{A}_{(2)} = \{a_* \in \mathcal{A}_s : Z^{(s,a_*)} \succeq_{(2)} Z^{(s,a')}, \forall a' \in \mathcal{A}_s \setminus \{a_*\}\}$.

When is it possible to apply the SSD policy? The following proposition describes a necessary requirement on return distributions for valid application.

Proposition 1. *Assume μ has two finite moments. Then $X \succeq_{(2)} Y$ if, and only if $\mu_X^{(1)} \geq \mu_Y^{(1)}$ or $\mu_X^{(1)} = \mu_Y^{(1)}$ and $\mu_X^{(2)} \leq \mu_Y^{(2)}$, where (\cdot) denotes a particular moment of the distribution μ .*

This implies that actions are ranked according to their mean, unless there is a tie - in which case the second moment is used. Furthermore, Prop 1 demands that any learning algorithm emits distributions with the correct first two moments - otherwise SSD orderings may be invalid. Moving forward we seek distributional learning algorithms that we know converge in the first two moments. This can be achieved knowing the return distribution converges to its target in the Wasserstein distance.

3.1 Wasserstein convergence

The k -th order Wasserstein distance for any two univariate measures $\mu, \nu \in \mathcal{P}(\mathbb{R})$, is defined as

$$\mathcal{W}_k(\mu, \nu) = \inf_{\gamma \in \mathcal{P}_k(\mu, \nu)} \left\{ \int_{\mathbb{R}^2} |x - y|^k d\gamma(x, y) \right\}^{1/k},$$

where $\mathcal{P}_k(\mu, \nu)$ is the set of all joint distributions with marginals μ and ν having k finite moments. The distance describes an optimal transport problem, where one seeks to transform μ to ν with minimum cost (Villani, 2008). The cost here is $|x - y|^k$. The \mathcal{W}_k distance is appealing as a distributional learning objective, because its convergence implies convergence in the first k moments (Villani, 2008).

Lemma 1. *Let $\mu_t, \mu \in \mathcal{P}(\mathbb{R}^d)$ and $k \geq 1$, then $\mathcal{W}_k(\mu_t, \mu) \rightarrow 0$ as $t \rightarrow \infty$ if, and only if $\mu_t \rightarrow \mu$ and $\mu_t^{(k)} \rightarrow \mu^{(k)}$, where (k) denotes the k -th moment.*

The Wasserstein distance is a central concept of distributional RL. Bellemare et al. (Bellemare et al., 2017) first showed the distributional Bellman operator contracts in the supremal Wasserstein distance. They proposed a discrete-measure approximation algorithm (CDRL) using a fixed mesh in probability space and later showed their approximation converges in \mathcal{W}_2 (Rowland et al., 2018). This implies CDRL could support SSD action selection. Less is understood about related methods that approximate the return distribution with a set of particles (Dabney et al., 2018, 2017). Only when the particles are fit to a mesh of quantiles is it known that \mathcal{W}_1 is minimized (Dabney et al., 2017). But it is still not clear if the SSD rule would yield valid comparisons here, since many distributions can realize the same mean but have starkly different second moments.

3.2 Distributional RL as free-energy minimization

We propose an alternative way to learn the return distribution while minimizing \mathcal{W}_2 . We cast the distributional RL problem as a free-energy minimization in terms of the functional

$$E(\mu) = F(\mu) + \beta^{-1}H(\mu). \quad (6)$$

Here, F is the potential, H is the entropy, and $\beta \in \mathbb{R}_+$ an inverse temperature parameter.

The potential energy defines what it means for a distribution to be optimal. We choose the low-energy equilibrium to coincide with minimum expected Bellman error, formed from (5). Energy is minimized when the mapping \mathcal{T} reaches its fixed point, $\mathcal{T}\mu^{(s,a)} = \mu^{(s,a)}$ for some (s, a) . Given a transition sample (s, a, r, s') , we compute the distributional targets $\mathcal{T}z^{(s,a)}$, which denote realizations of $\mathcal{T}\mu^{(s,a)}$, and define Bellman's potential energy as

$$F(\mu) = \frac{1}{2} \int \left(\mathcal{T}z^{(s,a)} - z^{(s,a)} \right)^2 d\mu = \int U(z) d\mu. \quad (7)$$

Many RL inference frameworks enjoy the benefits of energy-based models (Haarnoja et al., 2017; Zhang et al., 2018). Given the functional form of our potential, we can describe the optimal probability measure in closed form, as the Gibbs measure $\mu_*(z) = \mathcal{Z}^{-1} \exp\{-\beta U(z)\}$, where $\mathcal{Z} = \int \exp\{-\beta U(z)\} dz$.

3.3 The Fokker-Planck Equation

We would like to understand the convergence behavior of return distributions as the free-energy is minimized. Systems of this nature are typically modeled as continuous-time stochastic diffusion processes, where the distributions $\{\mu_t\}_{t \in [0,1]}$ evolve over a smooth manifold of probability measures from $\mathcal{P}_2(\mathbb{R})$. The dynamics of μ_t obey a diffusive partial differential equation called the Fokker-Planck equation:

$$\partial_t \mu_t = \nabla \cdot \left(\mu_t \nabla \left(\frac{\delta E}{\delta \mu_t} \right) \right). \quad (8)$$

Here, the sub-gradient with respect to time is denoted ∂_t , and the first variation (Gâteaux derivative) of free energy $\frac{\delta E}{\delta \mu}$. The Fokker-Planck equation plays a central role in statistical physics, chemistry, and biology. In the framing of optimization procedures, (8) dictates the solution path, or gradient flow, of μ as it evolves over the manifold of probability measures. This is captured in the following.

Proposition 2. Let $\{\mu_t\}_{t \in [0,1]}$ be an absolutely-continuous curve in $\mathcal{P}_2(\mathbb{R})$. Then for $t \in [0, 1]$, the vector field $\mathbf{v}_t = \nabla(\frac{\delta E}{\delta t}(\mu))$ defines a gradient flow on $\mathcal{P}_2(\mathbb{R})$ as $\partial_t \mu_t = -\nabla \cdot (\mu_t \mathbf{v}_t)$, where $\nabla \cdot \mathbf{u}$ is the divergence of some vector \mathbf{u} .

The free-energy functional, E , intuitively characterizes the diffusion and thus, the optimization landscape of our new distributional RL problem. Convergence to an optimal point can be guaranteed provided E is convex. By inspection, we know this to be the case for the return distribution μ in (6).

3.4 Discrete Time Solutions

We adopt an iterative procedure (Jordan et al., 1998) to approximately solve the gradient flow problem (8). The method discretizes time in steps of h and applies the proximal operator

$$\text{Prox}_{hE}^{\mathcal{W}}(\mu_k) = \underset{\mu \in \mathcal{P}_2(\mu, \mu_k)}{\text{argmin}} \mathcal{W}_2^2(\mu, \mu_k) + 2hE(\mu). \quad (9)$$

For every step k , the operator generates a path of distributions $\{\mu_t\}_{t=1}^K$ such that $\mu_{k+1} = \text{Prox}_{hE}^{\mathcal{W}}(\mu_k)$ is equivalent to μ_K . In contrast with the distributional Bellman operator (5), the proximal operator regulates Bellman minimization directly with \mathcal{W}_2 . And because E is convex in μ , this method obtains the unique solution to (8). This result is due to Jordan et al. (Jordan et al., 1998):

Proposition 3. Let $\mu_0 \in \mathcal{P}_2(\mathbb{R})$ have finite free energy $E(\mu_0) < \infty$, and for a given $h > 0$, let $\{\mu_t^{(h)}\}_{t=1}^K$ be the solution of the discrete-time variational problem (9), with measures restricted to $\mathcal{P}_2(\mathbb{R})$, the space with finite second moments. Then as $h \rightarrow 0$, $\mu_K^{(h)} \rightarrow \mu_T$, where μ_T is the unique solution of (8) at $T = hK$.

Furthermore, one can evaluate the free-energy (7) over the solution sequence and observe it becomes a decreasing function of time (a Lyapunov function). The result implies that the expected distributional Bellman error is minimized when using the JKO approach.

Proposition 4. Let $\{\mu_k^{(h)}\}_{k=0}^K$ be the solution of the discrete-time variational problem (9), with measures restricted to $\mathcal{P}_2(\mathbb{R})$, the space with finite second moments. Then $E(\mu_k)$ is a decreasing function of time.

Finally, we can show an equivalence between the output of our free-energy optimization (9) and the solution obtained from the optimal distributional Bellman operator (5).

Proposition 5. Let $\mu \in \mathcal{P}_2(\mathbb{R})$. If $\mathcal{T}\mu = \mu$, then $\text{Prox}_{hE}^{\mathcal{W}}(\mu) = \mu$ as $\beta \rightarrow \infty$.

4 Discrete Measure Solutions

Our goal is to numerically compute solutions to (9). Direct application of (9) is infeasible, because the $\{\mu_k\}$ are infinite-dimensional objects. We propose a discrete-measure approximation of μ using a Lagrangian (particle-based) discretization, where the measure is supported on N equally-likely diracs $\mu_k \approx \frac{1}{N} \sum_{i=1}^N \delta_{z_k^{(i)}}$. Given an initial set of particles at some state-action pair $z(s, a) = \{z^{(1)}, \dots, z^{(N)}\}$, we evolve them forward in time with steps of h to obtain the solution at $t + h$. We apply a finite number of gradient steps to approximate the convergence limit $T = hK$.

Following prior work (Cuturi, 2013; Peyré, 2015; Zhang et al., 2018), we lump the entropy term from E into \mathcal{W}_2^2 . Let $\mu = \sum_{i=1}^N \mu_i \delta_{x^{(i)}}$ and $\nu = \sum_{j=1}^N \nu_j \delta_{y^{(j)}}$ be finite distributions. Then the entropic-regulated \mathcal{W}_2^2 distance is

$$\mathcal{W}_\beta(\mu, \nu) = \inf_{P \in \mathbb{R}_+^{N \times N}} \langle P, C \rangle + \beta \text{KL}(P | \mu \otimes \nu), \text{ s.t. } \sum_{j=1}^N P_{ij} = \mu_i, \sum_{i=1}^N P_{ij} = \nu_j.$$

Here, $\langle P, C \rangle$ denotes the Frobenius norm between the joint P and the square Euclidean cost $C_{ij} = (x_i - y_j)^2$, and $\text{KL}(P | \mu \otimes \nu) = \sum_{i,j} [P_{ij} \log(P_{ij}/\mu_i \nu_j) - P_{ij} + \mu_i \nu_j]$. The entropic term promotes numerical stability by acting as a barrier function in the positive octant. JKO stepping under this new distance is denoted

$$\text{Prox}_{hF}^{\mathcal{W}_\beta}(\mu_k) = \underset{\mu \in \mathcal{P}_2(\mu, \mu_k)}{\text{argmin}} \mathcal{W}_\beta(\mu, \mu_k) + 2hF(\mu). \quad (10)$$

One can compute the entropic-regularized distance, \mathcal{W}_β , using Sinkhorn’s algorithm (Sinkhorn, 1967; Peyré and Cuturi, 2018; Cuturi and Doucet, 2014), which is a standard procedure we detail in the supplement. One can also consider parametric models for the particles, and apply auto-differentiation to back-propagate gradient information through the Sinkhorn procedure into the model. Our experiments use this approach with a tabular representation. A study of more sophisticated, neural particle models is left to future work.

4.1 SSD action selection with discrete measures

We want to compare discrete measures comprised of N equally-likely diracs for SSD action selection. Given the measures of two random returns, the SSD relation (1) checks the integrated CDFs, $F^{(2)}(\alpha)$, for every $\alpha \in \mathbb{R}$, which is numerically intractable. We circumvent this problem using cumulative quantile functions, $F^{-2}(\tau) = \int_0^\tau F^{-1}(t)dt$, assuming $F_Y^{-2}(0) = 0$, and $F_Y^{-2}(1) = \infty$:

$$X \succeq_{(2)} Y \iff F_X^{-2}(\tau) \geq F_Y^{-2}(\tau) \forall \tau \in (0, 1). \quad (11)$$

Notice that $F_X^{-2}(\tau)/\tau = \mathbf{E}[X|X \leq \xi^{(\tau)}]$ is the Conditional Value at Risk (CVaR) for level τ . Thus, the SSD condition can be interpreted as a continuum of CVaR constraints for risk levels $\tau \in (0, 1)$. This connection suggest a numerical way to compute the cumulative quantile function F^{-2} .

Lemma 2. *Let $\tau \in (0, 1)$ and consider $\xi^{(\tau)} = F_X^{-1}(\tau)$. Then $F_X^{-2}(\tau) = \mathbf{E}[X \leq \xi^{(\tau)}]$.*

Lemma 2 makes it possible to compare total expectations on subsets of the return space, instead of dealing with probability integrals over an unbounded domain.

Computations simplify even further when we consider finite sets of returns. Denote the ordered coordinates of a return distribution: $z^{[1]} \leq z^{[2]} \leq \dots \leq z^{[N]}$. Then given particle sets for two returns which were induced by actions a_1 and a_2 , we have

$$\begin{aligned} Z^{(s,a_1)} \succeq_{(2)} Z^{(s,a_2)} &\iff \mathbf{E}[Z^{(s,a_1)} \leq \xi_{a_1}^{(\tau)}] \geq \mathbf{E}[Z^{(s,a_2)} \leq \xi_{a_2}^{(\tau)}], \forall \tau \in (0, 1); \\ &\sum_{i=1}^j z_{a_1}^{[i]} \geq \sum_{i=1}^j z_{a_2}^{[i]}, \forall j = 1, \dots, N. \end{aligned} \quad (12)$$

Our algorithm uses (12) to find the safest action. The policy is implemented by checking (12) for all $\binom{|A_s|}{2}$ pairs with quantiles derived empirically from the particles. When dominance cannot be established (Fig. 2c), our policy returns the greedy action. Thus our policy strictly improves the greedy policy in risky domains. Values are straightforward to compute with equally-likely particles: $Q^{(s,a)} = \frac{1}{N} \sum_{i=1}^N z^{(i)}$.

4.2 The Dominant Particle Agent

Now we introduce the Dominant Particle Agent (DPA). The agent (Alg.1) selects actions according to the SSD behavior policy, denoted here with the operator \mathcal{B}_s for state s , and updates return distributions with the greedy action. This ensures the agent explores with risk-sensitive actions and learns the optimal policy. The proximal loss is computed in Alg.2 using the expected squared Bellman error and Sinkhorn’s algorithm for \mathcal{W}_β , which we detail in the supplement.

Algorithm 1 Dominant Particle Agent (Tabular)

- 1: # Initialize particles
 - 2: $z(s, a) = \{z^{(i)}\}_{i=1}^N \forall (s, a) \in \mathcal{S} \times \mathcal{A}$
 - 3: **for** $t = 1, 2, \dots$ **do**
 - 4: # Explore with the SSD behavior policy
 - 5: $s', r \sim p(\cdot|s, a)$ with $a \leftarrow \mathcal{B}_s z$
 - 6: # Exploit with the greedy target policy
 - 7: $a^* \leftarrow \arg \max_{a \in \mathcal{A}} \{\frac{1}{N} \sum_i z^{(i)}(s', a)\}$
 - 8: $\mathcal{T}z^{(i)} \leftarrow r + \gamma z^{(i)}(s', a^*) \forall i \in [N]$
 - 9: # Update particles with proximal step
 - 10: $z(s, a) \leftarrow \operatorname{argmin}_z L_{hF_{\mathcal{T}}}^{\mathcal{W}_\beta}(z, z(s, a))$
-

Algorithm 2 Proximal Loss

- 1: **input:** Source and target particles $z, z_0; \mathcal{T}z$
 - 2: $F_{\mathcal{T}}(z) \leftarrow \frac{1}{2N} \sum_{i=1}^N [\mathcal{T}z^{(i)} - z^{(i)}]^2$
 - 3: $\mathcal{W}_\beta(z, z_0) \leftarrow \text{Sinkhorn}_\beta(z, z_0)$
 - 4: # Output JKO loss
 - 5: **output:** $L_{hF_{\mathcal{T}}}^{\mathcal{W}_\beta} = \mathcal{W}_\beta(z, z_0) + 2hF_{\mathcal{T}}(z)$
-

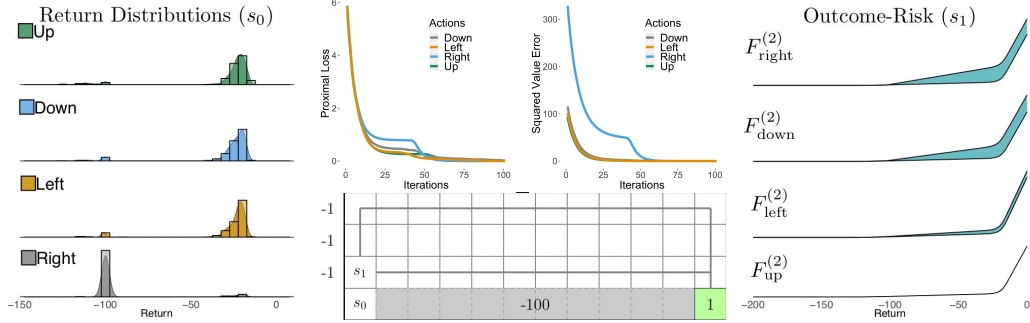


Figure 3: **Safe learning in the CliffWalk domain:** The left plot shows the DPA estimated histograms of the target densities. Convergence of the proximal loss and squared value error for each action are shown in the top two plots. The right plot arranges outcome-risk diagrams in descending order with respect to their dispersion space size. Although moving right is optimal, results indicate $a = \text{up}$ is the safest decision. Consequently, this is the action DPA takes.

5 Connections with Related Work

Particle-based Distributional RL: Particle models have been explored primarily with deep neural networks, in empirical studies. The QR-DQN agent trains a DQN network (Mnih et al., 2015) to output return particles on a fixed grid of quantiles (Dabney et al., 2017), which are constructed to minimize \mathcal{W}_1 with their targets. The IQN agent (Dabney et al., 2018) extends QR-DQN by training a sampling network that mimics the target distribution. These methods perform impressively well in complex Atari environments, where the state-space is high-dimensional. Our method also uses a particle representation, but in the tabular setting where we can offer formal guarantees about convergence. In the future, it would be interesting to compare these methods with a deep parametric variant of DPA.

Wasserstein Gradient Flows in RL: This space is relatively new. DP-WGF (Zhang et al., 2018) models stochastic policy inference as free-energy minimization, and applies the JKO scheme to derive a policy gradient algorithm. Their method is couched within the soft- Q learning paradigm (Haarnoja et al., 2017, 2018). These algorithms train a deep parametric model to sample from a target Gibbs density using Stein Variational Gradient Descent (Liu and Wang, 2016). In contrast, our method fixes a set of particles and adopts the more traditional Sinkhorn algorithm from Optimal Transport to compute the Wasserstein distance. Our method differs significantly in how it completes the JKO step using gradient methods and auto-differentiation.

Wasserstein minimization: The Wasserstein distance has become as a compelling objective in Machine Learning (Arjovsky et al., 2017; Chen et al., 2018). Its introduction to deep RL (Bellemare et al., 2017) spurred research that focuses on improving empirical performance on Atari benchmarks (Barth-Maron et al., 2018; Hessel et al., 2018). Though the exact reason for observed improvements remain an open area of research, evidence suggests the distributional model improves generalization (Imani and White, 2018). Our paper considers WGFs as they apply to Distributional RL.

Risk Modeling: Proposition 1 reveals a connection to the popular Markowitz mean-variance risk model (Markowitz, 1952). This can mislead one to think variance - the centralized second moment - sufficiently captures a distribution’s dispersion. Variance easily fails, however, when the distribution is not symmetric (Ogryczak and Ruszczyński, 2002). Better risk metrics such as VaR and CVaR model distributional geometry in the tails (Chow and Ghavamzadeh, 2014; Chow et al., 2017; Morimura et al., 2010; Rockafellar and Uryasev, 2000), but reflect risk only for a single specified level. The SSD measure captures distributional geometry at all risk levels, and thus provides a superior metric for action selection.

6 Experiments and Discussion

In this section we verify several prior assertions. Namely, we show the optimization procedure in Alg. 1 minimizes the proximal loss (10) to recover the latent return distribution. We also quantify the

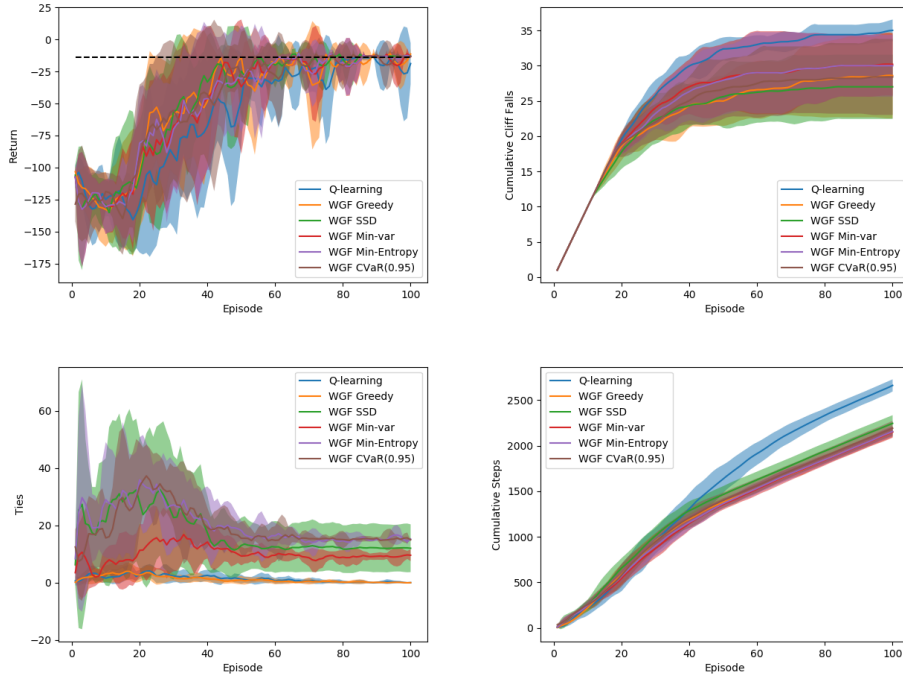


Figure 4: **Cliffwalk Results:** Performance (top left) of the different policies is statistically similar, since they all learn the same target policy. The cumulative safety metric (top right) shows some statistical differences between the SSD policy and Q-learning’s ϵ -greedy policy. Ties (bottom left) represent the number of times each non-greedy decision criterion was invoked. The cumulative performance in terms of steps (bottom right) shows the SSD policy makes the fewest mistakes but takes more steps to reach the goal.

agent’s ability to mitigate risk in a policy learning setting. In doing so, we draw comparisons with other baselines.

6.1 Solving the Gradient Flow Problem

Proposition 4 argues that repeated application of the proximal step (9) produces a decreasing function of time, implying that free energy is minimized at convergence. Here, we verify this is indeed the case by learning the return distribution from fixed targets obtained through Monte Carlo (MC) estimation.

The problem is set within the CliffWalk domain (Fig. 3). The transition dynamics follow those in Sutton & Barto (Sutton and Barto, 1998). We additionally include a five-percent chance of falling off the cliff from adjacent states. The optimal policy using the fewest steps, starts from s_0 , moves up, then along the cliff, until moving down brings the agent to the goal.

We show the convergence of the proximal loss and the mean square value error in Figure 3. The target distribution was obtained by rolling out a SARSA policy 200 times from s_0 . As we can see, the estimated distribution accurately captures the target’s features: the near certainty of walking off the cliff when moving right, the added chance of doing the same when choosing left or down, and finally the most profitable choice, moving up. In all experiments, we fix $\beta^{-1} = 0.5$ and $h = 0.05$.

6.2 Learning in the Presence of Risk

This experiment tasks the agent to learn a full CliffWalk policy from transition data. We study how optimality and risk are balanced throughout this training process. We compare several exploration policies that all break ties with a measure of distributional risk. These include SSD, variance, entropy, and CVaR. Several risk levels were analyzed for the CVaR policy. Here we present the 95 percent level and include results of the others in the supplement. We also included Q-learning as a familiar baseline for performance. Results are shown in Fig. 6. All agents used 32 particles.

6.3 Conclusion

We introduced SSD as a means for risk-sensitive action selection when using a distributional agent. We described DPA, a new WGF-based Distributional RL algorithm and showed how it balances risk and performance well in a setting with risk-optimality tradeoffs.

References

- Ambrosio, L. (2005). *Gradient Flows in Metric Spaces and in the Space of Probability Measures*. Lectures in Mathematics ETH Zurich.
- Arjovsky, M., Chintala, S., and Bottou, L. (2017). Wasserstein generative adversarial networks. In *Proceedings of the 34th International Conference on Machine Learning (ICML)*.
- Barth-Maron, G., Hoffman, M., Budden, D., Dabney, W., Horgan, D., TB, D., Muldal, A., Heess, N., and Lillicrap, T. (2018). Distributed distributional policy gradients. In *International Conference on Learning Representations (ICLR)*.
- Bellemare, M., Dabney, W., and Munos, R. (2017). A distributional perspective on reinforcement learning. In *Proceedings of the 34th International Conference on Machine Learning (ICML)*.
- Bellman, R. (1957). *Dynamic Programming*. Princeton University Press, Princeton, NJ, USA, 1 edition.
- Borkar, V. (2002). Q-learning for risk-sensitive control. *Mathematics of Operations Research*.
- Chen, C., Zhang, R., Wang, W., Li, B., and Chen, L. (2018). A unified particle-optimization framework for scalable bayesian sampling. *CoRR*.
- Chow, Y. and Ghavamzadeh, M. (2014). Algorithms for cvar optimization in mdps. In *Proceedings of the 27th International Conference on Neural Information Processing Systems (NIPS)*.
- Chow, Y., Ghavamzadeh, M., Janson, L., and Pavone, M. (2017). Risk-constrained reinforcement learning with percentile risk criteria. *Journal of Machine Learning Research*, 18.
- Cuturi, M. (2013). Sinkhorn distances: Lightspeed computation of optimal transport. In *Proceedings of the 26th International Conference on Neural Information Processing Systems (NIPS)*.
- Cuturi, M. and Doucet, A. (2014). Fast computation of wasserstein barycenters. In *Proceedings of the 31st International Conference on Machine Learning (ICML)*.
- Dabney, W., Ostrovski, G., Silver, D., and Munos, R. (2018). Implicit quantile networks for distributional reinforcement learning. In *Proceedings of the 35th International Conference on Machine Learning (ICML)*.
- Dabney, W., Rowland, M., Bellemare, M., and Munos, R. (2017). Distributional reinforcement learning with quantile regression. In *Proceedings of the Thirty-First AAAI Conference on Artificial Intelligence*.
- Dentcheva, D. and Ruszczyński, A. (2006). Inverse stochastic dominance constraints and rank dependent expected utility theory. *Mathematical Programming*.
- Fishburn, P. (1964). *Decision and Value Theory*. Wiley.
- Fishburn, P. (1980). Stochastic dominance and moments of distributions. *Math. Operations Research*.
- Haarnoja, T., Tang, H., Abbeel, P., and Levine, S. (2017). Reinforcement learning with deep energy-based policies. In *Proceedings of the 34th International Conference on Machine Learning (ICML)*.
- Haarnoja, T., Zhou, A., Abbeel, P., and Levine, S. (2018). Soft actor-critic: Off-policy maximum entropy deep reinforcement learning with a stochastic actor. In *Proceedings of the 35th International Conference on Machine Learning (ICML)*.

- Hessel, M., Modayil, J., van Hasselt, H., Schaul, T., Ostrovski, G., Dabney, W., Horgan, D., Piot, B., Azar, M. G., and Silver, D. (2018). Rainbow: Combining improvements in deep reinforcement learning. In *Proceedings of the Thirty-Second AAAI Conference on Artificial Intelligence*.
- Imani, E. and White, M. (2018). Improving regression performance with distributional losses. In *Proceedings of the 35th International Conference on Machine Learning (ICML)*.
- Jordan, R., Kinderlehrer, D., and Otto, F. (1998). The variational formulation of the fokker–planck equation. *SIAM Journal on Mathematical Analysis*.
- Liu, Q. and Wang, D. (2016). Stein variational gradient descent: A general purpose bayesian inference algorithm. In *Advances in Neural Information Processing Systems 29*.
- Markowich, P. and Villani, C. (1999). On the trend to equilibrium for the fokker-planck equation: An interplay between physics and functional analysis. In *Physics and Functional Analysis, Matematica Contemporanea (SBM) 19*.
- Markowitz, H. (1952). Portfolio selection. *Journal of Finance*.
- Mnih, V., D., K. K., Silver, Rusu, A., Veness, J., Bellemare, M., Graves, A., Riedmiller, M., Fidjeland, A., Ostrovski, G., Petersen, S., Beattie, C., Sadik, A., Antonoglou, I., King, H., Kumaran, D., D., W., Legg, S., and Hassabis, D. (2015). Human-level control through deep reinforcement learning. *Nature*.
- Morimura, T., Sugiyama, M., Kashima, H., Hachiya, H., and Tanaka, T. (2010). Parametric return density estimation for reinforcement learning. In *Proceedings of the Conference on Uncertainty in Artificial Intelligence*.
- Ogryczak, W. and Ruszczyński, A. (2002). Dual stochastic dominance and related mean-risk models. *SIAM J. on Optimization*.
- Peyré, G. (2015). Entropic approximation of Wasserstein gradient flows. *SIAM Journal on Imaging Sciences*.
- Peyré, G. and Cuturi, M. (2018). Computational optimal transport.
- Rockafellar, R. and Uryasev, S. (2000). Optimization of conditional value-at-risk. *Journal of Risk*.
- Rowland, M., Bellemare, M., Dabney, W., Munos, R., and Teh, Y. (2018). An analysis of categorical distributional reinforcement learning. In *International Conference on Artificial Intelligence and Statistics (AISTATS)*.
- Sato, M., Kimura, H., and Kobayashi, S. (2001). Td algorithm for the variance of return and mean-variance reinforcement learning. *Transactions of the Japanese Society for Artificial Intelligence*.
- Sinkhorn, R. (1967). Diagonal equivalence to matrices with prescribed row and column sums. In *The American Mathematical Monthly*.
- Sutton, R. and Barto, A. (1998). *Introduction to Reinforcement Learning*. MIT Press, 1st edition.
- Szepesvári, C. (2010). *Algorithms for Reinforcement Learning*. Morgan & Claypool.
- Tamar, A., Castro, D. D., and Mannor, S. (2013). Temporal difference methods for the variance of the reward to go. In *Proceedings of the 30th International Conference on Machine Learning (ICML)*.
- Villani, C. (2008). *Optimal Transport: Old and New*. Springer.
- von Neumann, J. and Morgenstern, O. (1947). *Theory of Games and Economic Behavior*. Princeton University Press.
- Zhang, R., Chen, C., Li, C., and Carin, L. (2018). Policy optimization as Wasserstein gradient flows. In *Proceedings of the 35th International Conference on Machine Learning (ICML)*.

7 Supplement

7.1 Proofs

All proofs are intended to apply for single measures.

Proposition 1. *Assume μ has two finite moments. Then $X \succeq_{(2)} Y$ if, and only if $\mu_X^{(1)} \geq \mu_Y^{(1)}$ or $\mu_X^{(1)} = \mu_Y^{(1)}$ and $\mu_X^{(2)} \leq \mu_Y^{(2)}$, where (\cdot) denotes a particular moment of the distribution μ .*

Proof. See Theorem 1 of (Fishburn, 1980). □

Lemma 1. *Let $\mu_t, \mu \in \mathcal{P}(\mathbb{R}^d)$ and $k \geq 1$, then $\mathcal{W}_k(\mu_t, \mu) \rightarrow 0$ as $t \rightarrow \infty$ if, and only if $\mu_t \rightarrow \mu$ and $\mu_t^{(k)} \rightarrow \mu^{(k)}$.*

Proof. See (Villani, 2008). □

Remark 1. *Let $E(\mu) = F(\mu) + \beta^{-1}H(\mu)$, with $F(\mu) = \int U(z)d\mu$. The minimizer is the Gibbs density,*

$$\mu_*(z) = Z^{-1} \exp\{-\beta\psi(z)\}, \quad (13)$$

where $\psi(z) = U(z) + \int_0^1 \lambda(\tau)S(z, \tau)d\tau$, and $Z = \int \exp\{-\beta\psi(z)\}dz$.

Proof. We set the functional derivative, or the first variation, of E to zero and solve for μ . The derivatives are

$$\frac{\delta F}{\delta \mu} = U(z), \quad \frac{\delta H}{\delta \mu} = \log(\mu) + 1.$$

Solving for μ_* emits a proportionality, which can be normalized as described:

$$U(z) + \beta^{-1}(\log(\mu_*) + 1) = 0 \implies \mu_* \propto \exp\{-\beta\psi(z)\}$$

□

Proposition 2. *Let $\{\mu_t\}_{t \in [0,1]}$ be an absolutely-continuous curve in $\mathcal{P}(\mathbb{R})$ with finite second-order moment. Then for $t \in [0, 1]$, the vector field $\mathbf{v}_t = \nabla(\frac{\delta E}{\delta t}(\mu))$ defines a gradient flow on $\mathcal{P}(\mathbb{R})$ as $\partial_t \mu_t = -\nabla \cdot (\mu_t \mathbf{v}_t)$, where $\nabla \cdot \mathbf{u}$ is the divergence of some vector \mathbf{u} .*

Proof. See (Ambrosio, 2005) Theorem 8.3.1. □

Proposition 3. *Let $\mu_0 \in \mathcal{P}_2(\mathbb{R})$ have finite free energy $E(\mu_0) < \infty$, and for a given $h > 0$, let $\{\mu_t^{(h)}\}_{t=0}^K$ be the solution of the discrete-time variational problem, with measures restricted to $\mathcal{P}_2(\mathbb{R})$, the space with finite second moments. Then as $h \rightarrow 0$, $\mu_K^{(h)} \rightarrow \mu_T$, where μ_T is the unique solution of the Fokker-Planck equation at $T = hK$.*

Proof. See (Jordan et al., 1998) Theorem 5.1. □

Proposition 4. *Let $\{\mu_t^{(h)}\}_{t=0}^K$ be the solution of the discrete-time JKO variational problem, with measures restricted to $\mathcal{P}_2(\mathbb{R})$, the space with finite second moments. Then $E(\mu_t)$ is a decreasing function of time.*

Proof. We show that the free-energy $E(\mu) = F(\mu) + \beta^{-1}H(\mu)$ is a Lyapunov functional for the Fokker-Planck (FP) equation. Following the approach of (Markowich and Villani, 1999), we consider the change of variables $\mu_t = h_t e^{-U}$, where we let $\beta = 1$ without loss of generality. With this, FP is equivalent to

$$\partial_t h_t = \Delta h_t - \nabla U \cdot \nabla h_t. \quad (14)$$

Whenever ϕ is a convex function of \mathbb{R} , one can check the following is a Lyapunov functional for (14), and equivalently the FP equation:

$$\int \phi(h_t) e^{-U} dz = \int \phi(\mu_t e^U) e^{-U} dz$$

Indeed

$$\frac{d}{dt} \int \phi(h_t) e^{-U} dz = - \int \phi''(h_t) |\nabla h_t|^2 e^{-U} dz < 0.$$

Now consider $\phi(h_t) = h_t \log(h_t) - h_t + 1$. With the identity $\int (h_t - 1) e^{-U} dz = 0$, we find

$$\begin{aligned} \int \phi(h_t) e^{-U} dz &= \int \mu_t \log\left(\frac{\mu_t}{e^{-U}}\right) dz, \\ &= \int \mu_t (U + \log \mu_t) dz = E(\mu). \end{aligned}$$

Thus, the free-energy functional is a Lyapunov function for the Fokker-Planck equation, and $E(\mu_t)$ is a decreasing function of time. In the low-energy state, when there is only pure Brownian motion, the optimal distributional Bellman equation is satisfied. \square

Proposition 5. *Let $\mu \in \mathcal{P}_2(\mathbb{R})$. If $\mathcal{T}\mu = \mu$, then $\text{Prox}_{hE}^{\mathcal{W}}(\mu) = \mu$ as $\beta \rightarrow \infty$.*

Proof. Let $d(\mu, \nu)$ be some distributional distance between measures μ and ν , such as the supremal k -Wasserstein $= \sup_{s,a} \mathcal{W}_k(\mu, \nu)$. Furthermore, suppose $\mu^* = \mathcal{T}\mu^*$ is the fixed point of the optimal distributional Bellman operator \mathcal{T} . We consider the proximal operator

$$\text{Prox}_{hE}^{\mathcal{W}}(\mu_k) = \underset{\mu}{\text{argmin}} \mathcal{W}_2^2(\mu, \mu_k) + 2hE(\mu).$$

It follows that $\mu^* = \mathcal{T}\mu^*$ and

$$\begin{aligned} d(\mathcal{T}\mu^*, \mu^*) &\leq d(\text{Prox}_{hE}^{\mathcal{W}}(\mu^*), \mu^*) = d\left(\underset{\mu}{\text{argmin}} \mathcal{W}_2^2(\mu, \mu^*) + 2h \underbrace{E(\mu)}_{0 \text{ as } \beta \rightarrow \infty}, \mu^*\right), \\ &\leq d\left(\underset{\mu}{\text{argmin}} \mathcal{W}_2^2(\mu, \mu^*) = \mu^*, \mu^*\right) \\ &\leq 0 \end{aligned}$$

Distance is non-negative, so it must be that $\text{Prox}_{hE}^{\mathcal{W}}(\mu^*) = \mathcal{T}\mu^* = \mu^*$. \square

Lemma 2. *Let $\tau \in (0, 1)$ and consider $\xi_\tau = F_X^{-1}(\tau)$. Then $F_X^{-2}(\tau) = \mathbf{E}[X \leq \xi_\tau]$.*

Proof. By conjugate duality,

$$\begin{aligned} F_X^{-2}(\tau) &= \tau \xi_\tau - F_X^{(2)}(x), \\ &= \tau \xi_\tau - \tau \mathbf{E}[X - \xi_\tau | X \leq \xi_\tau], \\ &= \tau \mathbf{E}[X | X \leq \xi_\tau], \\ &= \mathbf{E}[X \leq \xi_\tau]. \end{aligned}$$

\square

7.2 Sinkhorn's Algorithm

We describe how the Kantorovich problem can be made tractable through entropy regularization, then present an algorithm for approximating the \mathcal{W}_2^2 distance. The key message is that including entropy reduces the original Optimal Transport problem to one of matrix scaling. Sinkhorn's algorithm can be applied for this purpose to admit unique solutions.

The optimal value of the Kantorovich problem is the exact \mathcal{W}_2^2 distance. Given probability measures $\alpha = \sum_{i=1}^N \alpha_i \delta_{x_i}$ and $\beta = \sum_{j=1}^M \beta_j \delta_{y_j}$, the problem is to compute a minimum-cost mapping, π , defined as a non-negative matrix on the product space of atoms $\{x_1, \dots, x_N\} \times \{y_1, \dots, y_M\}$. Denoting the cost to move x_i to y_j as $C_{ij} = \|x_i - y_j\|^2$, we have

$$\mathcal{W}_2^2(\alpha, \beta) = \min_{\pi \in \mathbb{R}_{\geq 0}^{N \times M}} \langle \pi, C \rangle = \sum_{ij} \pi_{ij} C_{ij}, \quad (15)$$

$$\text{such that } \pi \mathbf{1}_M = \alpha, \pi^\top \mathbf{1}_N = \beta. \quad (16)$$

This approach constitutes a linear program, which unfortunately scales cubically in the number of atoms. We can reduce the complexity by considering an entropically regularized version of the problem. Let ε be a regularization parameter. The new problem is written in terms of the generalized Kullback Leibler (KL) divergence:

$$\mathcal{W}_2^2(\alpha, \beta) \approx \mathcal{W}_\varepsilon(\alpha, \beta) = \min_{\pi \in \mathbb{R}_{\geq 0}^{N \times M}} \langle \pi, C \rangle + \varepsilon \text{KL}(\pi \| \alpha \otimes \beta), \quad (17)$$

$$= \sum_{i,j} \pi_{ij} C_{ij} + \varepsilon \sum_{i,j} [\pi_{ij} \log \frac{\pi_{ij}}{\alpha_i \beta_j} - \pi_{ij} + \alpha_i \beta_j], \quad (18)$$

$$\text{such that } \pi \mathbf{1}_M = \alpha, \pi^\top \mathbf{1}_N = \beta. \quad (19)$$

The value of $\mathcal{W}_\varepsilon(\alpha, \beta)$ occurs necessarily at the critical point of the constrained objective function

$$L_\varepsilon = \sum_{i,j} \pi_{ij} C_{ij} + \varepsilon \sum_{i,j} [\pi_{ij} \log \frac{\pi_{ij}}{\alpha_i \beta_j} - \pi_{ij} + \alpha_i \beta_j] - \sum_i f_i \left(\sum_j \pi_{ij} - \alpha_i \right) - \sum_j g_j \left(\sum_i \pi_{ij} - \beta_j \right), \quad (20)$$

$$\frac{\partial L_\varepsilon}{\partial \pi_{ij}} = 0 \implies \forall i, j, C_{ij} + \varepsilon \log \frac{\pi_{ij}^*}{\alpha_i \beta_j} = f_i^* + g_j^*. \quad (21)$$

The last line of (21) shows that the entropically-regularized solution is characterized by two vectors $f^* \in \mathbb{R}^N, g^* \in \mathbb{R}^M$. With the following definitions

$$u_i = \exp(f_i^*/\varepsilon), \quad v_j = \exp(g_j^*/\varepsilon), \quad K_{ij} = \exp(-C_{ij}/\varepsilon), \quad (22)$$

we can write the optimal transport plan as $\pi^* = \text{diag}(\alpha_i u_i) K \text{diag}(v_j \beta_j)$. And the approximate Wasserstein distance can be computed simply as

$$\mathcal{W}_\varepsilon(\alpha, \beta) = \langle \pi^*, C \rangle + \varepsilon \text{KL}(\pi^* \| \alpha \otimes \beta) = \sum_{ij} (f_i^* + g_j^*) = \langle f^*, \alpha \rangle + \langle g^*, \beta \rangle$$

We mentioned that Optimal Transport reduces to positive matrix scaling. Indeed, using the vectors u and v , Sinkhorn's algorithm provides a way to iteratively scale K such that the unique solution is π^* . Initialize $u^{(0)} = \mathbf{1}_N$, and $v^{(0)} = \mathbf{1}_M$, then perform the following iterations for all i, j

$$\begin{aligned} v_j^{(1)} &= \frac{1}{[K^\top(\alpha \odot u^{(0)})]_j}, & u_i^{(1)} &= \frac{1}{[K(\beta \odot v^{(1)})]_i}, \\ \vdots & & \vdots & \\ v_j^{(n+1)} &= \frac{1}{[K^\top(\alpha \odot u^{(n)})]_j}, & u_i^{(n+1)} &= \frac{1}{[K(\beta \odot v^{(n+1)})]_i}. \end{aligned} \quad (23)$$

Sinkhorn's algorithm performs coordinate ascent with f and g to maximize the dual maximization problem

$$\mathcal{W}_\varepsilon(\alpha, \beta) = \max_{f \in \mathbb{R}^N, g \in \mathbb{R}^M} \langle f, \alpha \rangle + \langle g, \beta \rangle - \varepsilon \langle \alpha \otimes \beta, \exp\{(f \oplus g - C)/\varepsilon\} - 1 \rangle. \quad (24)$$

Each update consists of kernel products, $K^\top(\alpha \odot u)$ and $K(\beta \odot v)$, and point-wise divisions. We describe this procedure in Algorithm 3, using computations in the log domain to numerically stabilize the updates. The log updates derive from (22) and (25):

$$\begin{aligned} \log v_j &= -\log \sum_i K_{ij} \alpha_i u_i & \log u_i &= -\log \sum_j K_{ij} \beta_j v_j, \\ g_j &= -\varepsilon \log \sum_i \exp\{(-C_{ij} + f_i)/\varepsilon + \log \alpha_i\} & f_i &= -\varepsilon \log \sum_j \exp\{(-C_{ij} + g_j)/\varepsilon + \log \beta_j\}. \end{aligned} \quad (25)$$

The Sinkhorn iterations typically loop until convergence. In practice, we choose a decreasing temperature sequence $\{\varepsilon_n\}$ with which to bound the number of iterations.

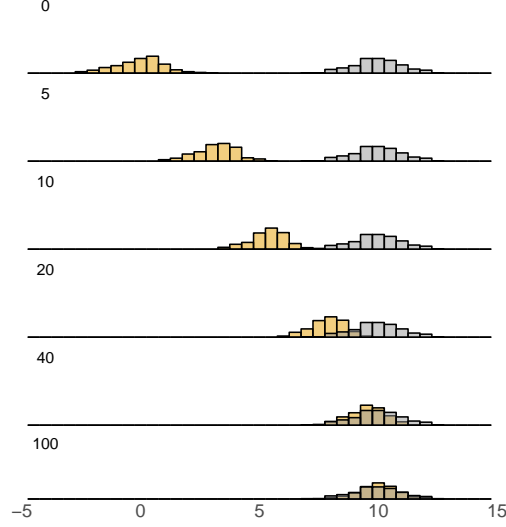


Figure 5: **Inference for a single target:** We transport a set of particles (gold) toward a target distribution (grey) by minimizing the proximal loss and computing the W_β with Sinkhorn’s algorithm. Six histograms are shown for 100 gradient steps.

Algorithm 3 Sinkhorn’s Algorithm in the log domain for W_2^2

- 1: **input:** Source and target measures $\alpha = \sum_{i=1}^N \alpha_i \delta_{x_i}, \beta = \sum_{j=1}^M \beta_j \delta_{y_j}$, Annealing temperature sequence $\{\varepsilon_n\}$
 - 2: # Initialize dual variables
 - 3: $i \in \{1, \dots, N\}, j \in \{1, \dots, M\}$
 - 4: $f_i \leftarrow 0, g_j \leftarrow 0 \forall i, j$
 - 5: # Perform coordinate ascent in the log domain
 - 6: **for** $\varepsilon \in \{\varepsilon_n\}$ **do**
 - 7: $C_{ij} = \frac{1}{2\varepsilon} \|x_i - y_j\|^2 \forall i, j$
 - 8: $g_j^{(n+1)} \leftarrow -\varepsilon \log \sum_i \exp\{(-C_{ij} + f_i^{(n)})/\varepsilon + \log \alpha_i\} \forall j$
 - 9: $f_i^{(n+1)} \leftarrow -\varepsilon \log \sum_j \exp\{(-C_{ij} + g_j^{(n+1)})/\varepsilon + \log \beta_j\} \forall i$
 - 10: # Return the entropic-regularized OT distance
 - 11: **output:** $\langle f, \alpha \rangle + \langle g, \beta \rangle$
-

7.3 Conditional Value at Risk Ablation Study

Here we vary the level at which conditional value at risk is measured and plot the average return, cumulative number of steps taken, cumulative number of cliff falls, and the number of tie breaks each method made.

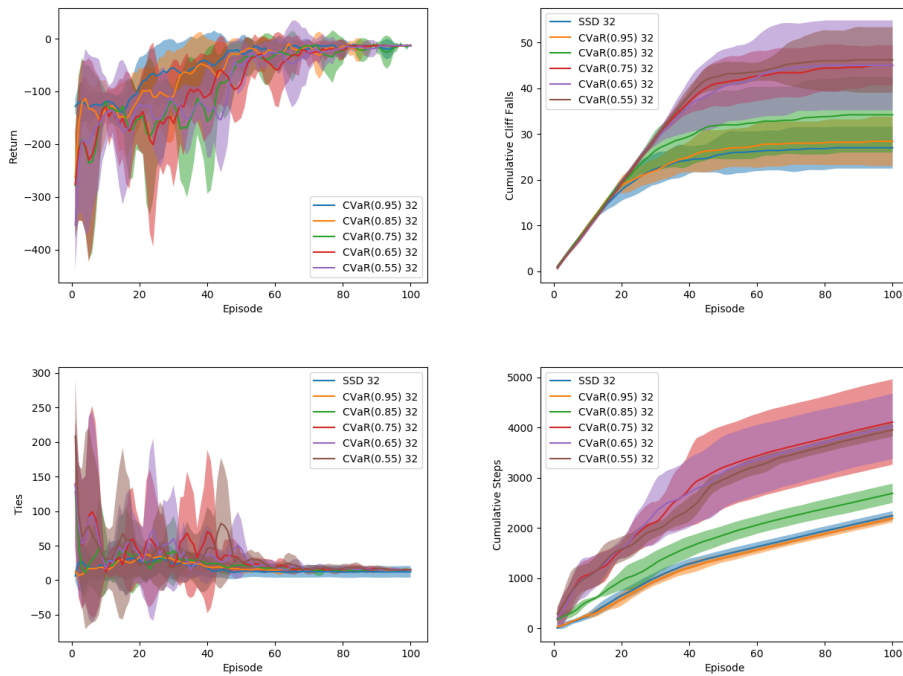


Figure 6: CVaR Results with 32 particles